DendroSync: An R package to unravel synchrony patterns in tree-ring networks

Josu G. Alday[a,*], Tatiana A. Shestakova[a,b], Víctor Resco de Dios[a], Jordi Voltas[a]

[a] *Department of Crop and Forest Sciences—AGROTECNIO Center, University of Lleida, Avda. Alcalde Rovira Roure 191, E-25198 Lleida, Spain*
[b] *Mathematical Methods and IT Department, Siberian Federal University, L. Prushinskoy St. 2, 660075 Krasnoyarsk, Russia*

A B S T R A C T

Spatial synchrony refers to the presence of a common signal for a time-varying characteristic that, in dendrosciences, is shared among tree-ring chronologies from a particular area. Analysis and interpretation of synchrony patterns in tree-ring networks is currently limited by: (i) the requirement for flexible modelling of complex correlations and heteroscedastic errors and (ii) the availability of ready-to-use open software to fulfil this task. We present an R package (DendroSync) that facilitates estimating and plotting synchrony patterns for pre-defined groups. The package has been devised to work with traits derived from tree rings (e.g. ring-width), but other data types are also suitable. It combines variance-covariance mixed modelling with functions that quantify the degree to which tree-ring chronologies contain a common signal over a fixed time period. It also estimates temporal changes in synchrony using a moving window algorithm. The functionality and usage of DendroSync are illustrated using a simple example.

1. Introduction

Dendrochronological archives provide long-term records of tree performance at varying spatial scales. The rising interest on the spatiotemporal dependence of forest dynamics on environmental cues has resulted in an increase of tree-ring networks worldwide (e.g. Barber et al., 2000; Briffa et al., 2002, 2008; Babst et al., 2013; St. George, 2014). These networks may contain complex patterns of coordinated (i.e. synchronous) temporal fluctuations in tree-ring signals. For instance, it has been reported that there is a common variation in regional tree-ring patterns engendered by correlated climatic forces and that the strength of this common variation diminishes with increasing distance. This phenomenon has received ample attention over the last decades (e.g. Fritts, 1976; Feliksik, 1993; Rolland, 2002; Frank and Esper 2005; Macias et al., 2006; Shestakova et al., 2016) and has been shown to be species- and region-specific (Di Filippo et al., 2007; Trouet et al., 2012; St. George, 2014; Shestakova et al., 2014, 2016). Hence, a natural question arises as to how such coordinated responses are structured across spatially disjunct stands (Rolland, 2002). Indeed, detailed analyses of coordinated patterns of tree-ring variability across geographical scales is likely to provide further insights into the influence of local and regional processes on the structure and function of forests. On the other hand, the available methodological approaches to unravel the complexities of tree-ring signals are still scarce.

In this context, spatial synchrony can be defined as the presence of a relevant common signal for a time-varying trait (e.g. ring-width) in a collection of tree-ring chronologies covering a particular area. Traditionally, the strength of the common signal shared by tree-ring series has been estimated through classical analysis of variance (ANOVA) (i.e. fixed effects model; Fritts, 1976). The seminal paper by Wigley et al. (1984) broadened the application of ANOVA in dendrosciences by establishing the theoretical background for estimating the uncertainty in the average common signal of a set of correlated series. Time series of indexed ring widths were described in terms of variance components of several random effects (Wigley et al., 1984). Indeed, tree-ring data are often better defined through a mixed model setting because of the associated random sources of variation, e.g. those associated with measurements repeated in time (Jennrich and Schluchter, 1986). Once the time (year) factor is taken as a random variable, inferences about the entire population of years can be derived from the estimation of the inter-annual variance common to a set of chronologies for a trait of interest. Hence, the proportion of common variance, or intra-class correlation, estimates the extent of coordinated (or synchronous) fluctuations among chronologies (Shestakova et al., 2014).

Synchrony patterns across geographical scales (i.e. from plots to continents) can be better disentangled and interpreted by grouping chronologies into potentially homogeneous subsets (e.g., Babst et al.,

2013; Shestakova et al., 2014). For instance, contrasting physiological responses between species or across regions may cause differential forest reactions to environmental conditions that remain registered in tree rings (de Luis et al., 2013; Galván et al., 2014). Factors such as phylogeny, geographical proximity or functional similarity may underlie different patterns of synchrony in a particular area. Shestakova et al. (2014) presented a mixed model framework to disentangle spatial patterns of tree-ring signals that was applied using proprietary software. This methodology allows assessing to what extent temporal responses are spatially structured by partitioning the variability associated to the time effect at intra- and inter-group levels. By applying different grouping criteria, temporal signals of different strength, shared within and between the subsets, can be quantified by variance-covariance mixed modelling. This framework has proved to be well suited to interpret synchrony patterns in tree-ring networks ranging from local (Shestakova et al., 2017) to sub-continental scales (Shestakova et al., 2016). However, broad analyses of such synchrony patterns are currently limited because of lack of non-proprietary software tools.

Despite their potential ecological applications, mixed models to study spatially structured tree-ring records are not yet broadly in use. Here, we present 'DendroSync' (Alday et al., 2017, CRAN: DendroSync), a package for the open-source R statistical environment (R Development Core Team, 2016) that facilitates the analysis and interpretation of synchrony patterns existing in tree-ring networks. DendroSync is based upon previously described methods (Shestakova et al., 2014). The package contains a suite of customizable functions that allow (i) evaluating and plotting complex patterns of synchrony for tree-ring traits over a given time period at within- and between-group levels that are pre-defined by the user and (ii) assessing temporal changes in those patterns using a moving window algorithm that divides the whole period of study into shorter sub-periods. We begin by describing the package functionality. We then provide an illustrative example and indicate where the package is available for download. Finally, we conclude by providing a general outlook of the package.

2. Package functionality

The package DendroSync quantifies synchrony across ring-width chronologies (or other tree-ring traits) for (i) a fixed time period defined by the user (i.e. at sub-centennial or centennial scales) and (ii) a moving time window that pre-defines intervals within the study period for which synchrony estimates are obtained independently (e.g. 30-year window). We note that this package can accommodate various time series datasets apart from tree rings, but it was originally devised to be used in a dendrochronological framework.

The package workflow is illustrated in Fig. 1. Following Shestakova et al. (2014, 2016), the package contains three function types: (i) functions to fit and, afterwards, select variance-covariance (VCOV) models based on goodness-of-fit statistics using a user-defined grouping criterion for any given tree-ring dataset; (ii) functions to calculate synchrony at within- and between-group levels from the selected VCOV models for the whole study period and (iii) functions to calculate temporal changes in synchrony using moving-window intervals across the time series. Appropriate plotting functions of synchrony patterns at within- and between-group levels for the whole period and of temporal changes in synchrony across sub-periods are also available. In total, 15 different functions are implemented, but nine are mainly for internal use (Fig. 1).

2.1. Data handling

The package DendroSync has been designed to work with residual indices of tree-ring width (TRW) chronologies that may partly overlap, hence covering a given period. To obtain indexed chronologies we recommend the use of high-pass filter algorithms. In this way, biological growth trends are eliminated while a common variance at inter-annual time scales is potentially preserved across chronologies (i.e. high-frequency variability related to climate or other external drivers of tree performance). The package can also handle other ecological data in which long-term trends and temporal autocorrelation have been previously removed (e.g. tree-ring traits such as isotopic series or density measurements, climatic time series, remote sensing derived data, etc.). The input data must be formatted as a data frame with TRW (response variable), time and grouping variables as columns. The time variable is used to specify the years to be included in the analyses, and the grouping variable defines the grouping criterion applied to stratify the dataset of chronologies into subsets for analysis of synchrony patterns at both within- and between-group levels. A variable coding for a chronology factor (Code) should also be included to account for the effect of series (fixed) in the model. However, if time series vary around the same mean (as in the case of indexed ring-width chronologies), the variable Code becomes redundant and can be saved. In this case, the model turns into a random effects model. Missing values can be reported as NA.

2.2. Variance-covariance model selection

The first step to calculate synchrony values of indexed TRW chronologies for a grouping variable over a fixed time period (Fig. 1) is the selection of the best VCOV model. The function dendro.varcov fits seven VCOV models relating TRW against specific names of tree-ring width chronologies (TRW ~ Code) or, alternatively, the VCOV models can be fitted without code identification of chronologies if they are centred on the same mean value (TRW ~ 1). Whatever the choice, time and grouping variables are modelled using positive-definite matrices (?pdClasses) to characterize synchrony for each level of the grouping variable and also across pairwise combinations of levels (i.e. within- and between-group synchrony). The function returns the following VCOV model outputs (Shestakova et al., 2014): a null positive-definite matrix structure (mBE; *broad evaluation*), and the homoscedastic and heteroscedastic (homoscedastic = TRUE or FALSE) versions of a diagonal positive-definite matrix structure (mNE, mHeNE; *narrow evaluation*), a positive-definite matrix with compound symmetry structure (mCS, mHeCS; *compound symmetry*) and a general positive-definite matrix structure (mUN, mHeUN; *unstructured*). Briefly, *broad evaluation* ignores the existence of groups so the year variance is constant at the within- and between-group levels; *narrow evaluation* tests for lack of common signals between chronologies belonging to different groups (i.e. covariances are set to zero); *compound symmetry* fits homogeneous year variances across groups and homogeneous covariances across pairwise combinations of groups; finally, *unstructured* allows for heterogeneous variances and covariances. The heteroscedastic variants of these VCOV models arise from allowing the residual variance to vary among groups. Afterwards, the function mod.table provides a table comparing VCOV models by Akaike's Information Criterion (AIC), corrected AIC (AICc) and Bayesian Information Criterion (BIC) in the smaller-is-better form (Burnham and Anderson, 2002). Based on these criteria the best fitting VCOV model can be selected from this table.

2.3. Synchrony estimation

The function sync estimates synchrony from a previously selected VCOV model, amongst those produced by dendro.varcov. A modname argument is included in sync function to select one among the seven models of interest (mBE, mNE, mHeNE, mCS, mHeCS, mUN, mHeUN). The output lists synchrony estimates at the within- and between-grouping variable levels, quantifying the degree to which the values of chronologies contain a common signal. A standard error (SE) of each synchrony estimate is also included. This output can be directly used as input for the sync.plot function where dot plots of within- and between-grouping variable synchrony are produced. These dot plots are used to
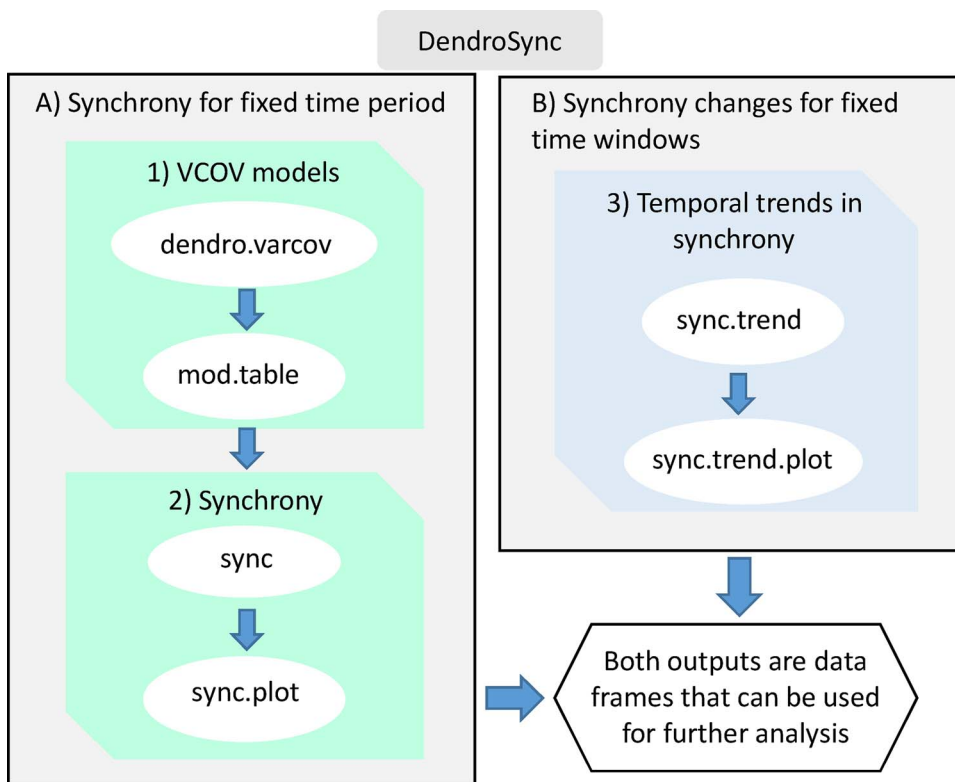
DendroSync

A) Synchrony for fixed time period

1) VCOV models

dendro.varcov

↓

mod.table

↓

2) Synchrony

sync

↓

sync.plot

B) Synchrony changes for fixed time windows

3) Temporal trends in synchrony

sync.trend

↓

sync.trend.plot

→ Both outputs are data frames that can be used for further analysis

Fig. 1. Workflow and overview of the main functions included in the package DendroSync. Two main approaches are described independently: A) calculating synchrony over a fixed time period and B) calculating temporal changes in synchrony for fixed time windows.

represent synchrony values (and their SEs) obtained for each level of grouping variable and also for pairwise combinations of levels (i.e. within- and between-group synchrony).

2.4. Temporal changes in synchrony using a moving time window

The function sync.trend provides information on changes in synchrony over time. This function estimates synchrony in TRW data for particular time periods using a moving time window as described in Shestakova et al. (2016). By default, the time variable is split in observation windows of 30 years that are lagged 5 years; the set of VCOV models fitted by dendro.varcov are then generated for each window. The sync.trend function uses the same data input as the dendro.varcov function. Afterwards, sync.trend chooses, for each time window, the best VCOV model based on the information criterion selected between "AIC", "AICc" or "BIC" (selection.method). Then, the selected model is used to calculate the within- or between- grouping variable levels synchrony for each time window.

The output of sync.trend function consists of a data frame indicating, for each time window, the best fit model, the information criterion used, the within- or between-group synchrony and the mean time point for each window (varTime). The function sync.trend is very flexible and can be customized using internal arguments. For example, the window width and lag can be specified using arguments window and lag respectively. Also, the user can customize the type of information criterion used for model selection (selection.method), whether the models are homoscedastic or heteroscedastic (homoscedastic), and whether between-group synchrony is evaluated or not (between.group). The sync.trend output can be directly used for plotting synchrony trends using the function sync.trend.plot. This plotting function creates line charts showing synchrony changes across selected time windows at the within- and between-group levels (and their standard errors as colour ribbons). One of the strengths of DendroSync is that either single period synchrony or synchrony trend outputs can be used in further analyses relating synchrony values to their potential external drivers, e.g. through linear mixed models or correlation analyses (for an example, see Shestakova et al., 2016).

3. Illustrative example

The package DendroSync includes a dataset of 30 tree-ring width chronologies of conifer species compiled from Shestakova et al. (2016). The sampling sites are distributed along a latitudinal gradient (*ca.* 37–43˚N) across Spain with the following species representation: *Abies alba* Mill., *Pinus nigra* subsp. *salzmannii* (Dunal) Franco and *Pinus sylvestris* L (Fig. 2). Residual TRW chronologies were obtained using standard dendrochronological techniques (Cook and Kairiukstis, 1990) and covered the period 1950–1999 (CRAN: DendroSync) (Fig. 2). Particularly, ring-width measurements were converted to site chronologies of ring-width indices by applying detrending and autocorrelation removal with the Friedman supersmoother spline (Friedman, 1984) and autocorrelation modelling. This procedure aimed at eliminating biological growth trends but preserving high-frequency variability potentially related to climate (Fritts, 1976).

This dataset can be potentially stratified following either taxonomic (i.e. species grouping) or geographic (i.e. regional grouping) criteria (Fig. 2). Synchrony patterns at species level have been previously reported in Shestakova et al. (2016). Instead, we use here the regional grouping to illustrate the functionality of the package. This analysis can be useful to evaluate whether warming-induced effects on forests (e.g. an increasing impact of drought) are homogenising climate responses of trees between and within regions, as previously reported at the local level for the Iberian peninsula (Shestakova et al., 2017). In this example, ring-width chronologies are classified into three groups according to their latitudinal position across Spain as follows: 'north' (14 sites), 'centre' (10 sites) and 'south' (6 sites). Here we characterize regional patterns of synchrony by (i) modelling between- and within-group variability over the whole length of TRW chronologies (1950–1999 period), and (ii) evaluating temporal changes in synchrony for successive time intervals over this period.
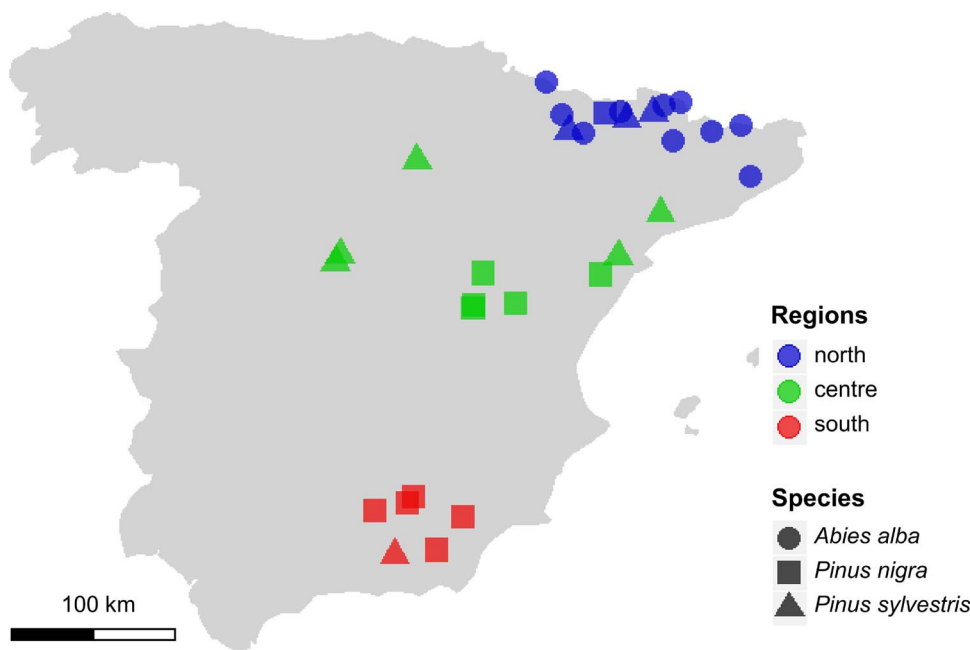
Fig. 2. Distribution of sampling sites across Spain. Coloured circles denotes regions: north (blue), centre (green) and south (red). Genus symbols are as follows: *Abies alba* (circle), *Pinus nigra* (square) and *Pinus sylvestris* (triangle). (For interpretation of the references to colour in this figure legend, the reader is referred to the web version of this article.)

3.1. Calculating synchrony over a fixed time period

In this section, we describe how synchrony is estimated at within- and between-group levels over the whole time span covered by the tree-ring chronologies (i.e. over a fixed time period; Fig. 1). First, the dataset, named 'conifersIP', should be called by typing data(conifersIP) in the R console (the first rows can be viewed using head(conifersIP)). After loading the data, restricted maximum likelihood (REML) estimation of variance components for each model is obtained using dendro.varcov function:

```
> data(conifersIP)
> head(conifersIP)
> ModHm < -  dendro.varcov(TRW ~ Code,  varTime = "Year",
varGroup = "Region", data = conifersIP, homoscedastic = TRUE)
> ModHt < -  dendro.varcov(TRW ~ Code,  varTime = "Year",
varGroup = "Region", data = conifersIP, homoscedastic = FALSE)
> mod.table(ModHm)
> mod.table(ModHt)
```

The formula argument of dendro.varcov relates TRW against specific names of tree-ring width chronologies (Code). Here, we can use a simplified model (TRW ~ 1) instead of fitting a Code effect since chronologies are centred on the same mean value. The output provided is in any case equivalent. The arguments varTime = "Year" (random term) and varGroup = "Region" (fixed term) indicates the variables used to fit the variance-covariance matrices. Homogeneity of residual variance is a main assumption of standard ANOVA, and conclusions on varTime × varGroup interactions may not be appropriate if this assumption is not fulfilled. The structure of error variances can be specified within the argument homoscedastic, which indicates whether homoscedastic (TRUE) or heteroscedastic (FALSE) variants of VCOV models should be fitted.

The output of this function, in this case named ModHm for homocedastic models and ModHt for heteroscedastic models, is a list containing information for each fitted model and can be directly used as input in mod.table. This function creates a table of restricted log-likelihood values for each model and derives goodness-of-fit criteria such as AIC, AICc and BIC (Table 1). Here, we consider models with substantial support to be those in which the difference of either AIC or BIC between models is < 2 (Raftery, 1996; Burnham and Anderson, 2002). This difference corresponds to the information loss experienced if using an alternative model instead of the best-fit model for inference (Burnham

Table 1
Variance-covariance model comparison for 30 tree-ring width chronologies from the Iberian Peninsula (as provided by DendroSync) according to restricted log-likelihood (LogLik) statistics: Akaike's Information Criterion (AIC), corrected AIC (AICc) and Bayesian Information Criterion (BIC). AIC, AICc and BIC are in smaller-is-better form. n is the number of observations used in the model fit and df is the degrees of freedom related with the number of parameters in the fitted model. The model of choice is shown in bold.

Model[*]	n	df	AIC	AICc	BIC	LogLik
Homoscedastic						
mBE	1461	32	−1301.6	−1300.2	−1133.1	−1365.6
mNE	1461	34	−1327.2	−1325.6	−1148.2	−1395.2
mCS	1461	34	−1369.9	−1368.3	−1190.9	−1437.9
mUN	1461	37	−1371.4	−1369.5	−1176.5	−1445.4
Heteroscedastic						
mBE	1461	32	−1301.6	−1300.2	−1133.1	−1365.6
mHeNE	1461	36	−1350.1	−1348.3	−1160.5	−1422.1
mHeCS	**1461**	**35**	**−1395.3**	**−1393.5**	**−1210.9**	**−1465.3**
mHeUN	1461	39	−1394.2	−1392.1	−1188.8	−1472.2

* Model abbreviations: Broad Evaluation model, mBE; Narrow Evaluation model, mNE; Compound Symmetry model, mCS; Unstructured model, mUN; heteroscedastic variant of mNE, mHeNE; heteroscedastic variant of mCS, mHeCS; heteroscedastic variant of mUN, mHeUN.

and Anderson, 2002).

In this example, the AIC and BIC criteria pointed to the presence of differential ring-width signals across the three regions because the null model (mBE), which ignores the presence of groups, obtained the least support (i.e., largest AIC and BIC values). Moreover, the narrow evaluation model (i.e. testing for lack of a common spatial signal shared across pre-defined groups) also showed higher AIC and BIC values (i.e. poorer fitting) relative to other alternative models that account for the presence of shared variability among groups. This was expected from previous work because trees growing in neighbouring regions are likely to share similar climatic influences, as shown for distances of up to 1000 km in the Iberian Peninsula (Shestakova et al., 2016). Instead, the compound symmetry model with heteroscedastic errors provided the best fit according to AIC and BIC (mHeCS, Table 1). This output suggests that the magnitude of common ring-width signals is region-dependent, since the residual variation was distinct for each group. It also indicates the presence of significant ring-width fluctuations that are common across regions.

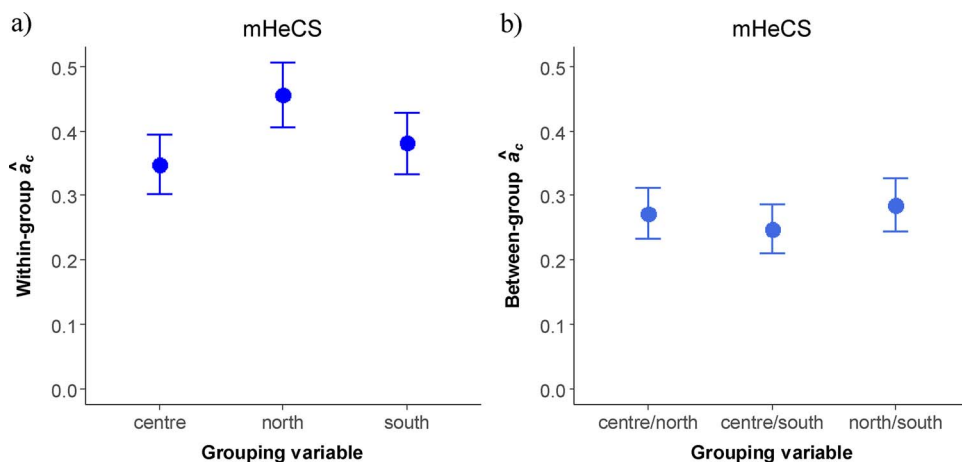The user selected model (mHeCS) is then used as input in sync

a) mHeCS
b) mHeCS

Fig. 3. Example of a dot plot created with the sync.plot function. Synchrony estimates ($\hat{a}_C$) for 30 tree-ring width chronologies originated from the Iberian Peninsula are calculated for the best variance-covariance model (see Table 1) at (a) within-group and (b) between-group levels over the period 1950–1999. Grouping of chronologies is based on geographic classification (north, centre and south). Error bars depict standard errors (SE).

function to derive estimates of synchrony at within- and between-group levels (referred to as $\hat{a}_C$, following Wigley et al., 1984 and Shestakova et al., 2014) for the corresponding VCOV structure:

> bestmod < - sync(ModHt, modname = "mHeCS")

Synchrony values can also be plotted using the following code:

> sync.plot(bestmod)

The sync function needs to include a dendro.varcov output object, here ModHt, to retrieve information on VCOV models, while the modname argument is needed to specify which model from ModHt is to be used to calculate synchrony, here "mHeCS". The sync output, in this case named bestmod, can be inspected for synchrony values or, instead, can be directly used as input in sync.plot to create within- and between-group synchrony dot plots with error bars (Fig. 3). In this example, the selected model (compound symmetry with heteroscedastic error variances) provides support for higher synchrony among chronologies of the north of Spain compared with those from the other two regions, hence suggesting a stronger climate forcing in the north. As expected, the extent of synchronous growth is lower at the between-region than at the within-region level; however, differences in between-region synchrony do not follow a pattern of geographic distance (i.e. more distant regions do not show less synchronous growth) (Fig. 3). Such patterns of common variability shared by TRW chronologies can provide valuable insights into the biogeographical organization of tree-ring signals. That is, through VCOV modelling one may test hypotheses on contrasting growth patterns across groups of chronologies that are known or that can be defined based on existing or *a priori* knowledge. In contrast, multivariate approaches (e.g. principal component or factor analysis) are widely used to infer *a posteriori* patterns of common growth in tree-ring networks, that is, based on the tree-ring records themselves (e.g. Peterson and Peterson 2001; Andreu et al., 2007).

For further analyses, $\hat{a}_C$ values over the whole time period derived from sync function can be accessed by typing "bestmod".
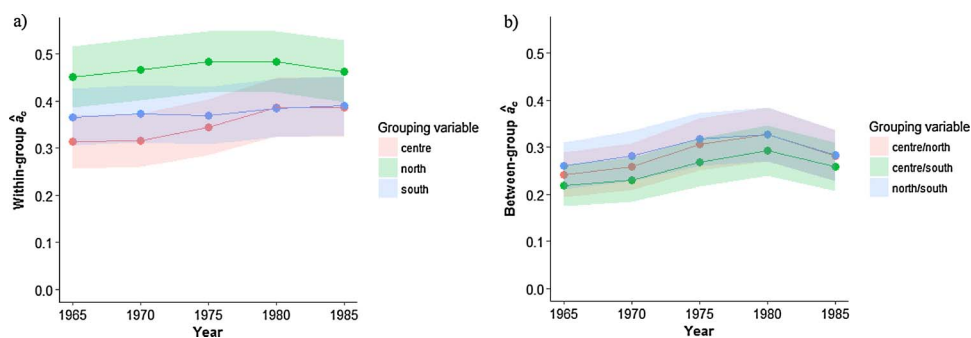
3.2. Calculating temporal changes in synchrony for fixed time windows

Temporal changes in synchrony can also be easily obtained and plotted by combining two functions: sync.trend and sync.trend.plot. An example code to execute these functions reads:

> reg.trend < -   sync.trend(TRW ~ Code,   varTime = "Year", varGroup = "Region",   homoscedastic = FALSE,   data = conifersIP, window = 30,   lag = 5,   null.mod = FALSE,   selection.method = c ("BIC"), all.mod = FALSE, between.group = FALSE)

> sync.trend.plot(reg.trend)

The first four function arguments of sync.trend are identical to those of dendro.varcov, namely the formula argument (TRW ~ Code), the time variable (varTime), the grouping variable (varGroup), and whether homoscedastic or heteroscedastic models should be defined (homoscedastic). In addition, the arguments window and lag are used to set the moving window interval and time lag over which the $\hat{a}_C$ values are calculated. By default, they are set to 30 and 5 years, respectively. The null.mod argument specifies whether only the broad evaluation model (TRUE) or also more complex VCOV structures (FALSE) will be evaluated. The selection.method argument indicates the goodness-of-fit criteria used to select the best VCOV model, here "BIC". The all.mod argument specifies whether both homoscedastic and heteroscedastic types of models are fitted in the same analysis (TRUE) or, instead, if only the type of models selected with the argument homoscedastic (homoscedastic or heteroscedastic) are fitted (FALSE). The first option is useful to assess changes in the structure of error variances of the fitted models over time.

The sync.trend output, a data.frame called "reg.trend" here, can be directly used to plot changes in synchrony with sync.trend.plot function. In this example, sync.trend.plot creates a plot showing temporal changes in synchrony at the within-group level (Fig. 4a). By setting the sync.trend argument between.group to TRUE, a plot showing between-group level temporal trends of $\hat{a}_C$ values is also produced (Fig. 4b). This function is useful to visualise changes in synchrony over time and at

a)
b)

Fig. 4. Example of a plot created with the sync.-trend.plot function. Synchrony estimates ($\hat{a}_C$) for 30 tree-ring width chronologies originated from the Iberian Peninsula at (a) within-group and (b) between-group levels are calculated for the best model for 30-year moving intervals lagged by 5 years over the period 1950–1999. The x-axis shows the central year of the moving time interval. Grouping of chronologies is based on geographic classification (north, centre and south). Shadows are standard errors (SE).

different levels (i.e. within and between groups). In this example, growth synchrony increases over the period 1950–1999 at the between-group level, suggesting a strengthening of drought-induced growth limitations (Shestakova et al., 2016) (Fig. 4b). At the within-group level, conversely, only the central region shows a slight increase in synchrony (Fig. 4a). For further analyses, temporal changes in $\hat{a}_C$ values across sub-periods derived from sync.trend function can be accessed by typing "reg.trend".

4. Package availability

DendroSync can be directly downloaded from the Comprehensive R Archive Network website (CRAN: https://CRAN.R-project.org/package=DendroSync). It can be installed from the R console by typing 'install.packages("DendroSync")' or, alternatively, by using the install packages menu. Once installed, users have access to the package documentation explaining the main package functions (Readme) and also to the reference manual (DendroSync.pdf) containing code examples for all functions. The package documentation is also accessible from the R console using the command '?any.function' (e.g. '?sync' to access sync function documentation and examples). DendroSync depends on the R packages "nlme" (CRAN: nlme; Pinheiro et al., 2016) and "ggplot2" (CRAN: ggplot2; Wickham, 2009).

5. Outlook

Unravelling the complexities of forest dynamics at large geographical scales is becoming a major priority of global-change research, and tree-ring records have emerged as very valuable data (Babst et al., 2017). DendroSync is a comprehensive tool to assess synchrony patterns from dendrochronological data using a set of customizable functions. Alternative R packages suitable for synchrony evaluation compute correlation matrices and related statistics such as variograms, and also plot spatial trends using correlograms (CRAN: Gouhier and Guichard, 2014, "synchrony" and Bjornstad, 2016, "ncf"). However, the main singularity of DendroSync is that it uses VCOV models to test for synchrony patterns within and between groups that are pre-defined by the user, thus providing synchrony estimates for the VCOV model that best approximates the data; besides, it plots temporal changes in synchrony within and between groups using a moving window algorithm. The DendroSync output can be complemented with the information generated by these alternative R packages, such as spatial correlograms as shown in Shestakova et al. (2016). The information provided by DendroSync can contribute to improve our understanding of how ecological factors determine tree performance across environmental gradients. Similarly to tree-ring traits, the package can handle other ecological records but the response variable should be previously corrected for long-term (e.g. inter-decadal) trends and autocorrelation. The outputs from synchrony functions are data-frames that can be used in further statistical analyses. Consequently, the DendroSync package, although tailored for the analysis of tree-ring records, is useful to unveil patterns of synchrony in miscellaneous ecological data using pre-defined grouping criteria. New functions and examples will be implemented in the future based on methodological refinements and suggestions of the research community (see https://josucham@bitbucket.org/josucham/dendrosync.git where development versions are available).

Acknowledgements

References

Alday, J.G., Shestakova, T.A., Resco de Dios, V., Voltas, J., 2017. DendroSync: Evaluating Synchrony from Dendrochronological Data. Package Version 0.1.0.

Andreu, L., Gutiérrez, E., Macias, M., Ribas, M., Bosch, O., Camarero, J.J., 2007. Climate increases regional tree-growth variability in Iberian pine forests. Global Change Biol. 13, 804–815.

Babst, F., Poulter, B., Trouet, V., Tan, K., Neuwirth, B., Wilson, R., Carrer, M., Grabner, M., Tegel, W., Levanič, T., Panayotov, M., Urbinati, C., Bouriaud, O., Ciais, P., Frank, D., 2013. Site- and species-specific responses of forest growth to climate across the European continent. Global Ecol. Biogeogr. 22, 706–717.

Babst, F., Poulter, B., Bodesheim, P., Mahecha, M.D., Franck, D.C., 2017. Improved tree-ring archives will support earth-system science. Nat. Ecol. Evol. 1, 0008.

Barber, V., Juday, G.P., Finney, B., 2000. Reduced growth of Alaska white spruce in the twentieth century from temperature-induced drought stress. Nature 405, 668–672.

Bjornstad, O.N., 2016. ncf: Spatial Nonparametric Covariance Functions. R package version 1. pp. 1–7. https://CRAN.R-project.org/package=ncf.

Briffa, K.R., Osborn, T.J., Schweingruber, F., Jones, P.D., Shiyatov, S.G., Vaganov, E.A., 2002. Tree-ring width and density data around the Northern Hemisphere: part 1, local and regional climate signals. Holocene 12, 737–757.

Briffa, K.R., Shishov, V.V., Melvin, T.M., Vaganov, E.A., Grudd, H., Hantemirov, R.M., Eronen, M., Naurzbaev, M.M., 2008. Trends in recent temperature and radial tree growth spanning 2000 years across northwest Eurasia. Phil. Trans. R. Soc. B : Biol. Sci. 363, 2271–2284.

Burnham, K.P., Anderson, D.R., 2002. Model Selection and Multi-model Inference: a Practical Information-theoretic Approach. Springer, New York 488 pp.

de Luis, M., Čufar, K., Di Filippo, A., Novak, K., Papadopoulos, A., Piovesan, G., Rathgeber, C.B.K., Raventós, J., Saz, M.A., Smith, K.T., 2013. Plasticity in dendroclimatic response across the distribution range of Aleppo pine (*Pinus halepensis*). PLoS One 8, e83550.

Di Filippo, A., Biondi, F., Čufar, K., de Luis, M., Grabner, M., Maugeri, M., Saba, E.P., Schirone, B., Piovesan, G., 2007. Bioclimatology of beech (*Fagus sylvatica* L.) in the Eastern Alps: spatial and altitudinal climatic signals identified through a tree-ring network. J. Biogeogr. 34, 1873–1892.

Feliksik, E., 1993. Teleconnection of the radial growth of fir (*Abies alba* Mill.) within central Europe. Dendrochronologia 11, 171–175.

Frank, D., Esper, J., 2005. Characterization and climate response patterns of a high-elevation, multi-species tree-ring network in the European Alps. Dendrochronologia 22, 107–121.

Friedman, J.H., 1984. A variable span smoother. Tech. Rep. LCS 5, 1–30.

Fritts, H.C., 1976. Tree Rings and Climate. Academic Press, London 567 pp.

Galván, J.D., Camarero, J.J., Ginzler, C., Buntgen, U., 2014. Spatial diversity of recent trends in Mediterranean tree growth. Environ. Res. Lett. 9, 084001.

Gouhier, T.C., Guichard, F., 2014. Synchrony: quantifying variability in space and time. Methods Ecol. Evol. 5, 524–533.

Jennrich, R.I., Schluchter, M.D., 1986. Unbalanced repeated-measures models with structured covariance matrices. Biometrics 42, 805–820.

Macias, M., Andreu, L., Bosch, O., Camarero, J.J., Gutiérrez, E., 2006. Increasing aridity is enhancing silver fir (*Abies alba* Mill.) water stress in its south-western distribution limit. Clim. Change 79, 289–313.

Peterson, D.W., Peterson, D.L., 2001. Mountain hemlock growth responds to climatic variability at annual and decadal time scales. Ecology 82, 3330–3345.

Pinheiro, J., Bates, D., DebRoy, S., Sarkar, D., Core Team, R., 2016. nlme: Linear and Nonlinear Mixed Effects Models. R Package Version 3. pp. 1–128. URL: http://CRAN. R-project.org/package=nlme.

R Development Core Team, 2016. R: A Language and Environment for Statistical Computing. R Foundation for Statistical Computing, Vienna, Austria.

Raftery, A.E., 1996. Approximate Bayes factors and accounting for model uncertainty in generalised linear models. Biometrika 83, 251–266.

Rolland, C., 2002. Decreasing teleconnections with inter-site distance in monthly climatic data and tree-ring width networks in a mountainous Alpine area. Theor. Appl. Climatol. 71, 63–75.

Shestakova, T.A., Aguilera, M., Ferrio, J.P., Gutiérrez, E., Voltas, J., 2014. Unravelling spatiotemporal tree-ring signals in Mediterranean oaks: a variance–covariance modelling approach of carbon and oxygen isotope ratios. Tree Physiol. 34, 819–838.

Shestakova, T.A., Gutiérrez, E., Kirdyanov, A.V., Camarero, J.J., Génova, M., Knorre, A.A., Linares, J.C., Resco de Dios, V., Sánchez-Salguero, R., Voltas, J., 2016. Forests synchronize their growth in contrasting Eurasian regions in response to climate warming. Proc. Natl. Acad. Sci. U. S. A. 113, 662–667.

Shestakova, T.A., Camarero, J.J., Ferrio, J.P., Knorre, A.A., Gutiérrez, E., Voltas, J., 2017. Increasing drought effects on five European pines modulate Δ13C-growthcoupling along a Mediterranean altitudinal gradient. Funct. Ecol 31, 1359–1370.

St. George, S., 2014. An overview of tree-ring width records across the Northern Hemisphere. Quat. Sci. Rev. 95, 132–150.

Trouet, V., Panayotov, M., Ivanova, A., Frank, D., 2012. A pan-European summer teleconnection mode recorded by a new temperature reconstruction from the north-eastern Mediterranean (AD 1768–2008). Holocene 22, 887–898.

Wickham, H., 2009. ggplot2: Elegant Graphics for Data Analysis. Springer-Verlag, New York, USA.

Wigley, T.M.L., Briffa, K.R., Jones, P.D., 1984. On the average value of correlated time series, with applications in dendroclimatology and hydrometeorology. J. Clim. Appl. Meteorol. 23, 201–213.